

Case Report

Acute Abdominal Distension Due to Disseminated Peritoneal Neoplasia in a Rhesus Macaque (*Macaca mulatta*)

Jennifer L Asher,¹ Grace J Barnett,² and Caroline J Zeiss^{1,*}

This report describes the clinical, radiographic, and pathologic findings in a female rhesus macaque that presented with acute abdominal distension and tympany. The macaque was euthanized after evidence of severe colonic distension on radiography and observation of widespread peritoneal adhesions on exploratory laparotomy. Gross and histopathologic evaluation revealed extensive entrapment of gastrointestinal and reproductive tracts by serosal fibrovascular proliferative tissue containing foci of endometriosis. The diagnosis of endometrial stromal sarcoma was supported by expression of CD10, Wilm tumor 1, estrogen receptor, and progesterone receptor and failure to express immunohistochemical markers characteristic of a range of differential diagnoses. In humans, this relatively uncommon neoplasm can arise from sites of endometriosis and often presents clinically as intestinal obstruction, similar to the presentation in this macaque.

Abbreviation: ESS, endometrial stromal sarcoma

DOI: 10.30802/AALAS-CM-17-000112

Acute abdominal distension and tympany occurs sporadically in both Old and New World NHP colonies and is most commonly associated with acute gastric dilatation.^{1,17,23} Predisposing factors include sudden changes in diet or feeding schedule, acute overfeeding, anesthetic events, and long-term antibiotic therapy that disrupts normal gastric flora.^{1,25} Most cases of gastric dilatation involve rapid production of gas by clostridial organisms, usually *Clostridium perfringens*, resulting in gastric distension and possible torsion.^{1,5,8,22} Early signs of gastric dilatation are hyperactivity or lethargy, agitation, dyspnea, abdominal rigidity, and gastric tympany. Due to the subtle nature of early signs and rapid disease course, the animal is often found dead or in a state of advanced cardiovascular compromise.²³ Emergency treatment is often unsuccessful but includes decompression of the stomach by using a large-bore stomach tube, appropriate treatment of shock, administration of antibiotics targeting clostridial and other anaerobes, parenteral fluid therapy, and careful monitoring for recurrence of condition.^{1,17}

Case Report

Three months prior to euthanasia, the 9-y-old, sexually intact female rhesus macaque in this report was scheduled for an ovariectomy after a presumptive diagnosis of endometriosis. This diagnosis was based on a history of painful menstrual cycling and uterine enlargement (approximate diameter, 5 cm) noted on routine examination. During surgery, adhesions

deep to the abdominal wall prevented full visualization of the abdominal cavity. Caudally, these adhesions were thick, fibrous, and firmly attached to the pelvic organs. Attempts to gain visualization resulted in hemorrhage from vessels buried within the adhesions as well as an incision into the bladder, which was adhered to the peritoneum. At that point, the procedure was discontinued, the bladder repaired, and the decision was made to treat the animal medically. She received medroxyprogesterone (40 mg IM; Depo-Provera, Pfizer, New York, NY) for treatment of endometriosis, the presumptive cause of the abdominal cavity abnormalities noted during surgery. Due to investigator concerns regarding medroxyprogesterone's reported effects on glucoregulatory function,^{11,15} no additional doses were administered, and alternative treatment options were being researched at the time of her presentation with abdominal distension. The macaque was seronegative for SIV, simian retrovirus, simian T-lymphotropic virus, and *Macacine herpesvirus 1* (Herpes B virus).

Three months after surgery, the macaque presented acutely with abdominal distension, anorexia, and lethargy. During the preceding 2 d, she was observed to be menstruating and partially anorexic but was otherwise bright, alert, and responsive. In light of her concurrent diagnosis of endometriosis and absence of other clinical signs, she was placed on medical observation, appetite monitoring, and meloxicam (0.1 mg/kg SC daily for 2 d). On the morning of the third day, the macaque was lethargic and completely anorexic, with marked abdominal distension and facial pallor. She was anesthetized (ketamine, 10 mg/kg IM; atropine, 0.05 mg/kg IM) for a full physical exam and diagnostic workup.

Physical examination revealed a taut, distended abdomen and pale mucous membranes with delayed capillary refill time. Her body temperature was low normal (99.8 °F [37.7 °C]); heart

Received: 17 Nov 2017. Revision requested: 26 Dec 2017. Accepted: 22 Jan 2018.

¹Department of Comparative Medicine, Yale School of Medicine, New Haven, Connecticut, and ²Comparative Medicine Resources, Rutgers University, New Brunswick, New Jersey

*Corresponding author. Email: caroline.zeiss@yale.edu

and respiratory rates were both elevated, at 178 bpm and 40 breaths per minute, respectively. Abdominal auscultation revealed diffuse abdominal tympany. Supportive oxygen was provided through a nose cone, and 250 mL of lactated Ringer solution was administered intravenously over 30 min. An endotracheal tube was placed, and an orogastric tube was passed. Small amounts of liquid and solid food material were collected from the orogastric tube, with minimal reduction of the abdominal distension. Radiographs revealed a decrease in serosal detail within the abdominal cavity, food material and gas were present in the stomach, and the large intestine was severely gas-distended (Figure 1). An enema was attempted but was unsuccessful because the tube could not be passed more than 5 cm into the rectum. An intravenous bolus of 5% dextrose was started, and the macaque's facial color improved, but mucous membranes appeared injected.

Primary differential diagnoses after radiographs included intestinal tympany secondary to bacterial dysbiosis, intraluminal, or extraluminal gastrointestinal obstruction. Due to the inability to resolve the abdominal distension by using medical therapy and the anticipated decline in the macaque's cardiovascular stability, emergency laparotomy was performed. Approximately 200 mL of serosanguinous fluid was suctioned from the peritoneal cavity. Extensive fibrohemorrhagic adhesions were present throughout the abdominal cavity, resulting in almost complete adhesion and fusion of the intestinal and reproductive tracts. Given her poor prognosis after recovery from anesthesia, the macaque was euthanized by using intravenous barbiturate overdose while she was still anesthetized.

Gross pathology. Thickened, vascularized omentum and serosa adhered the stomach and bowel loops to the urinary bladder and reproductive tract (Figure 2). The proliferative peritoneal tissue had a heterogeneous reddened appearance due to regions of frank hemorrhage and multiple, variably sized fibrovascular regions associated with small clear or blood-filled cysts. These changes were most evident in the caudal abdomen in association with the urinary bladder, reproductive tract, and terminal intestinal tract. Intestinal pathology was most severe in the descending colon and rectum: these regions were completely adhered to one another resulting in marked and fixed deviations of anatomy (Figure 2). Anterior to these areas, the large intestine was markedly dilated. Gross sectioning of the entire intestine revealed no breach of the mucosa (lesions were limited to the serosal layer) and no evidence of mucosal neoplasia. The urinary bladder and reproductive tract displayed a similar fibrovascular serosal reaction with many associated small cysts (Figure 2). No significant pathology was noted in other organs.

Histopathology. All peritoneal serosal surfaces were covered by abundant fibrovascular tissue. The cysts apparent during necropsy corresponded histologically to spaces containing blood or serous fluid or clusters of detached cells embedded within the fibrovascular tissue (Figure 3 A). These blood-filled spaces were lined by pleomorphic polygonal cells that were variably confluent with the surrounding spindle population (Figure 3 B). In addition, similar cells were arranged as nodules or sheets that extended through fibrovascular tissue to the peritoneal surface. In some areas, these cells assumed a polygonal shape with well-defined cytoplasmic membranes, variably abundant extracellular matrix, and granular intracytoplasmic material that stained positively after periodic acid-Schiff staining. Moderate anisocytosis and anisonucleosis were present, and the mitotic rate was low (that is, fewer than 1 mitosis per

high-power field). A vigorous peritoneal mesothelial response was evident.

Both ovaries were encased in a thick sheet of tissue located exterior to the cortex (Figure 4 A and B). This tissue predominantly was composed of polygonal to spindle cells with well-defined cytoplasmic membranes and granular intracytoplasmic material stained positively after periodic acid-Schiff staining. Moderate anisocytosis and anisonucleosis were present, and the mitotic rate was low (that is, fewer than 1 mitosis per 40× field). Isolated simple cuboidal to columnar glandular structures resembling endometrial glands were embedded within the periovarian tissue (Figure 4 B), which was continuous with stroma of adjacent ovarian endometriomas. Scattered mononuclear cells with granular brightly eosinophilic cytoplasm, consistent with NK cells, were distributed throughout. Clearly differentiated foci of endometriosis were scattered throughout omental fat, fibrovascular tissue, and connective tissue surrounding ovaries, oviduct, and uterus. The uterus demonstrated endometrial changes consistent with menses.

Immunohistochemistry. Clearly differentiated endometriomas consistent with peritoneal endometriosis were interspersed within the prevailing serosal fibrovascular reaction containing blood-filled spaces lined by pleomorphic polygonal cells. This presentation supported consideration of severe peritoneal endometriosis as a primary differential. However, we felt that the extent and severity of the peritoneal proliferative response in this animal warranted consideration of additional differential diagnoses, including peritoneal extension of intestinal carcinoma, mesothelioma, hemangiosarcoma, leiomyosarcoma, gastrointestinal stromal tumor, endometrial stromal sarcoma (ESS), and peritoneal extension of a malignant ovarian process. Immunohistochemical comparison of peritoneal and ovarian lesions with well-defined endometriomas is given in Table 1.

The periovarian proliferative tissue contained small numbers of well-defined pancytokeratin (AE1/AE3)-positive epithelial-lined cysts (Figure 4 A) embedded within cytokeratin (AE1/3 and CK5/6)-negative stromal tissue. Stromal tissue was positive for vimentin and smooth-muscle actin and expressed markers typical of endometrial stroma (CD10, progesterone receptor; Figure 4 C and E). This immunohistochemical phenotype, the continuity of periovarian tissue with ovarian endometriosis (Figure 4 A), and histologic features consistent with decidualized stroma supported the conclusion that the periovarian tissue was mesenchymal in origin and most likely derived from stromal elements of adjacent endometriosis.

We also immunohistochemically explored the origin of the nodular and blood-filled cystic lesions within the fibrovascular proliferative peritoneal response (Table 1 and Figure 3). These lesions were variably positive for smooth-muscle actin and desmin, failed to express epithelial markers, and expressed markers indicative of stromal tissues of reproductive origin (CD10, Wilm tumor 1, estrogen receptor, and progesterone receptor). All peritoneal proliferative tissue was immunonegative for CD117, a marker of gastrointestinal stromal tumor. Proliferative fibrovascular serosal tissue was robustly vascularized and composed predominantly of spindle cells with periodic epithelioid appearance on serosal surfaces. Greater anisocytosis was evident in the epithelioid regions on serosal surfaces, but the mitotic rate was still low (fewer than 1 mitosis per 40× field). Both spindle and epithelioid cells had a biphasic immunophenotype, expressing both mesenchymal (smooth-muscle actin and desmin) and broad-spectrum epithelial (cytokeratin AE1/AE3) markers, but not CK5/6. Proliferative peritoneal tissue was negative for a mesothelioma marker, calretinin. Endothelial

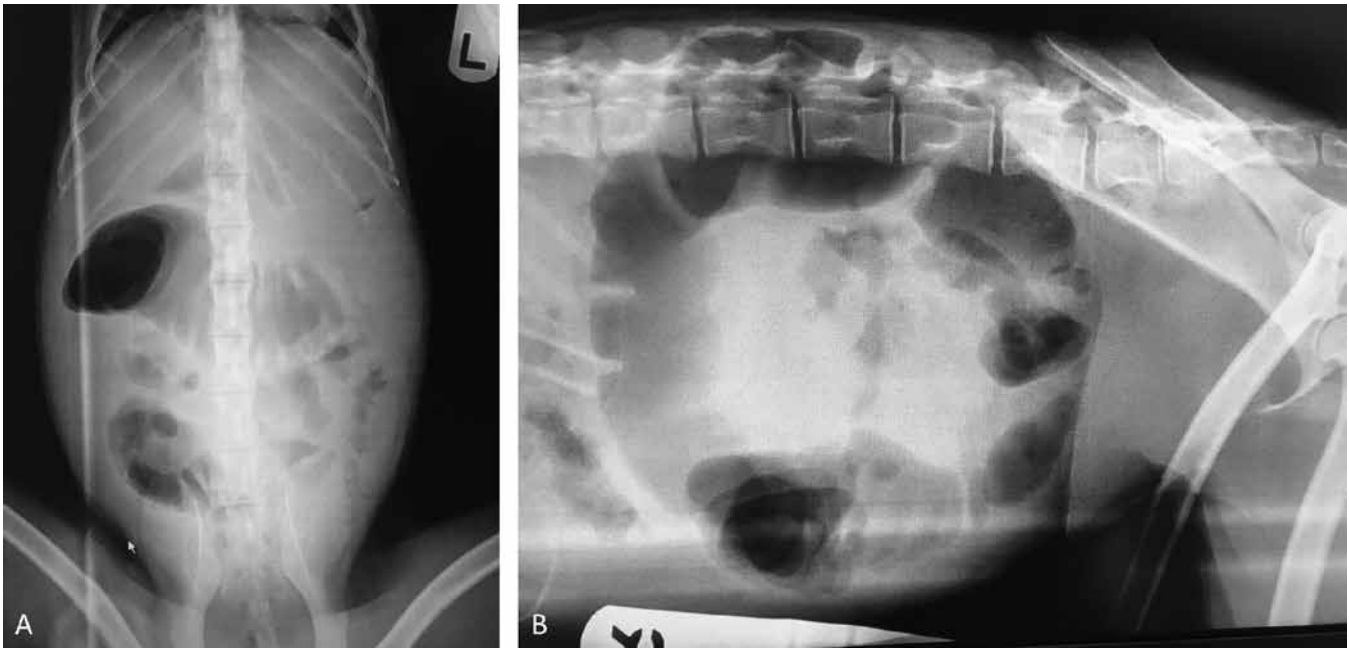


Figure 1. Radiographic findings. (A) Ventrodorsal and (B) right lateral radiographs shows decreased serosal detail throughout the abdominal cavity. The stomach appears to be in its normal position and filled with food material. The orogastric tube end is visible in both views. The large intestine is severely distended with gas, which appears in greater detail in right lateral radiographic view (B).

markers factor VII-related antigen and Wilm tumor (a marker of reactive vasculature) identified well-formed vessels through the fibrovascular response but not within nodular or cystic lesions. In summary, nodular and blood-filled cystic lesions within the fibrovascular proliferative peritoneal response presented an immunohistochemical phenotype consistent with stromal tissue of reproductive origin.

Discussion

The potential origins of the proliferative fibrovascular peritoneal lesions in this case are broad. Because the macaque had evidence of endometriosis and ovarian pathology, the peritoneal lesions might represent a vigorous response to endometriosis, malignant transformation of endometrial stroma (ESS), or a reactive process associated with ovarian neoplasia. Sclerosing peritonitis associated with the ovarian neoplasia luteinized thecoma has been described in humans^{4,26} but not NHP. Given the prevalence of intestinal carcinoma in rhesus macaques, we strongly considered carcinomatosis originating from a neoplastic enteric lesion. Mesothelioma was another possibility, and the highly vascularized nature of the peritoneal response prompted consideration of hemangiosarcoma. Additional differential diagnoses included retroperitoneal fibromatosis,²⁹ leiomyosarcoma, gastrointestinal stromal tumor, and idiopathic sclerosing peritonitis.²

Periovarian lesions were bilateral and composed of stromal tissue that was located exterior to the ovarian cortex. Similar to this macaque case, thecomas accompanied by sclerosing peritonitis are typically bilateral, demonstrate variably plump spindle to polygonal morphology, and express progesterone and estrogen receptor.^{4,26} However, unlike this case, thecomas arise within the cortex and usually express calretinin and cytokeratin.^{4,26} In our case, continuity of this tissue with regions of clear ovarian endometriosis, histologic features of decidualized endometrial stroma surrounding glands, and an immunohistochemical profile consistent with stromal tissues of reproductive origin (CD10, Wilm tumor 1, estrogen receptor,

and progesterone receptor) support the conclusion that periovarian tissue was derived from ovarian endometriosis.

Peritoneal lesions were characterized by a vigorous fibrovascular and mesothelial reaction comprising numerous blood-filled cystic structures lined by pleomorphic polygonal cells that were variably confluent with the surrounding fibrovascular tissue. These cells expressed immunohistochemical markers similar to those noted in endometrial stroma and periovarian tissue (negative for cytokeratin AE1/AE3; positive for smooth-muscle actin, CD10, Wilm tumor, estrogen receptor, and progesterone receptor). Carcinomatosis of enteric origin was excluded through careful gross dissection of the gastrointestinal tract, the lack of gross or histologic evidence of adenocarcinoma, and the failure of nodular and cystic lesions to express broad-spectrum cytokeratin.

Retroperitoneal fibromatosis is characterized by proliferation of spindle cells accompanying inflammatory cell infiltrates, fibroblasts, and endothelial cells subjacent to the pleura and peritoneum.¹ This abnormality occurs in conjunction with progressive immunodeficiency caused by infections with simian retrovirus 2 or the rhadinovirus known as retroperitoneal fibromatosis herpesvirus.²⁹ Our macaque did have fibrovascular cell proliferation, but showed no evidence of immunodeficiency or lymphoid depletion, and she tested negative for simian retrovirus 2 annually throughout her life. In addition, in highly cellular proliferative lesions of retroperitoneal fibromatosis, 25% to 75% of cells stain positive for factor VIII-related antigen. In our macaque, factor VIII-related antigen immunoreactivity was noted only in well-differentiated vascular profiles, consistent with vascularization secondary to the primary proliferative process.¹³

Hemangiosarcoma, leiomyosarcoma, and gastrointestinal stromal tumor were excluded on the basis of histologic characteristics and immunohistochemical results. Spindle cells within fibrovascular tissue interspersed between blood-filled cystic structures variably expressed both mesenchymal markers (smooth-muscle actin, desmin) and occasionally

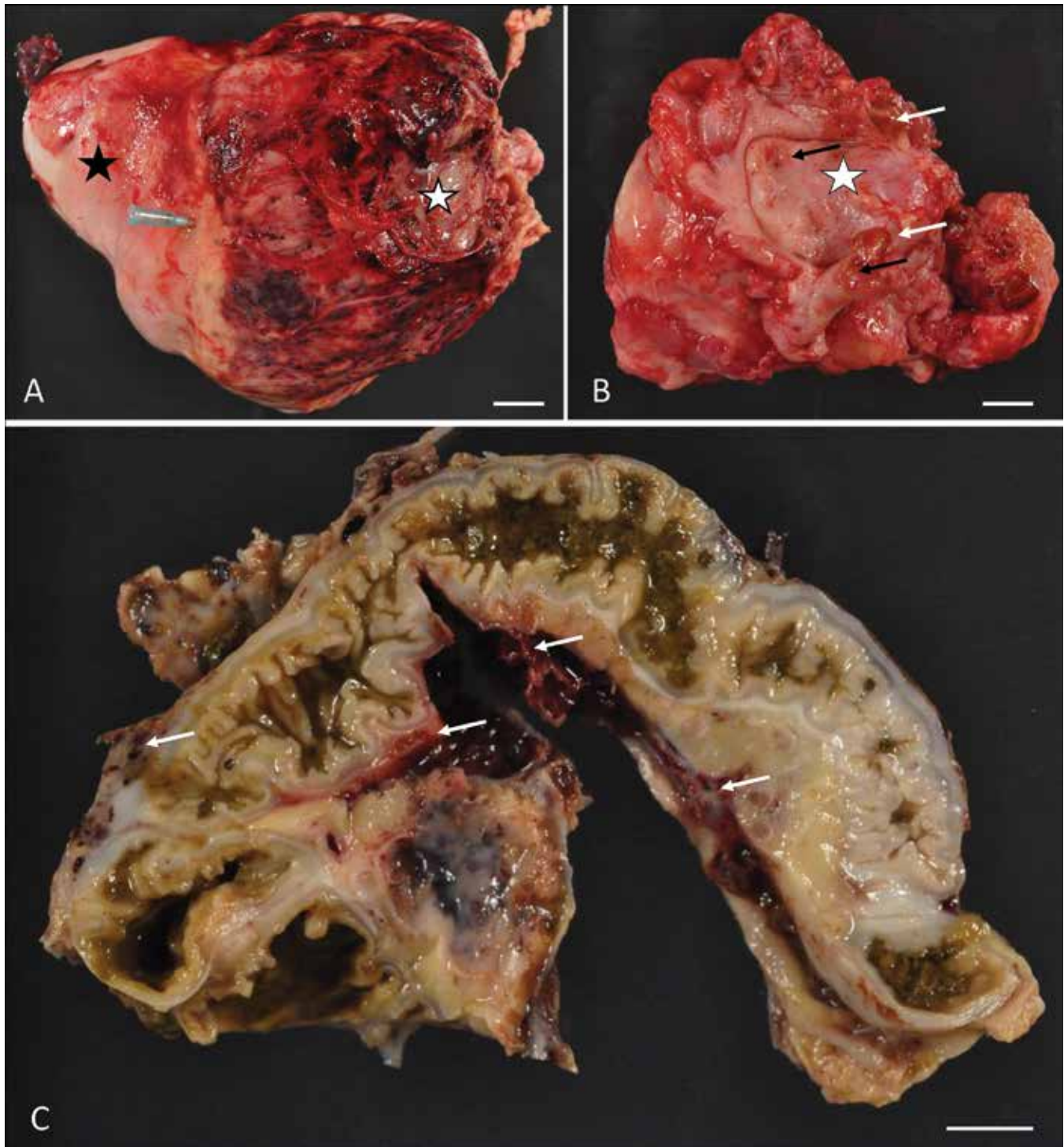


Figure 2. Gross pathology. (A) Intestinal tract, ventral view. Large and small intestines are coiled into an adherent mass covered by highly vascularized and hemorrhagic omentum and serosa. Omental lesions are most severe toward the caudal aspect of the abdomen. The location of the reproductive tract (removed) is indicated with a white asterisk. The stomach (black asterisk) is relatively unaffected. A catheter placed during surgery in an attempt to deflate the intestinal tract is located in the colon. (B) Reproductive tract, dorsal view. The dorsal aspect of the uterus (asterisk), ovaries (white arrows) and surrounding proliferative tissue are shown. Grossly visible uterine and ovarian endometriotic cysts are present (black arrows). (C) Terminal colon and rectum, longitudinal section. The intestinal lumen is partly occluded and demonstrates sharp deviations imposed by proliferative tissue limited to serosa (white arrows). The rectum is located at the lower right of the image. Bar, 1 cm.

broad-spectrum cytokeratin, consistent with mesothelial proliferative lesions due to various causes including mesothelioma.^{9,14}

These findings narrowed our differential list to severe endometriosis, ESS, and mesothelioma. Calretinin immunoreactivity frequently accompanies both epithelioid and spindle variants of mesothelioma;^{9,27} in our macaque, peritoneal tissue was

negative for this marker. Endometriosis is the presence of both endometrial glands and stroma outside the uterus, and is the most common reproductive disorder in Old World NHP. Risk of developing endometriosis increases with age, and there is also evidence of genetic susceptibility inherited through familial lines.³⁰ The disease may be asymptomatic, but common

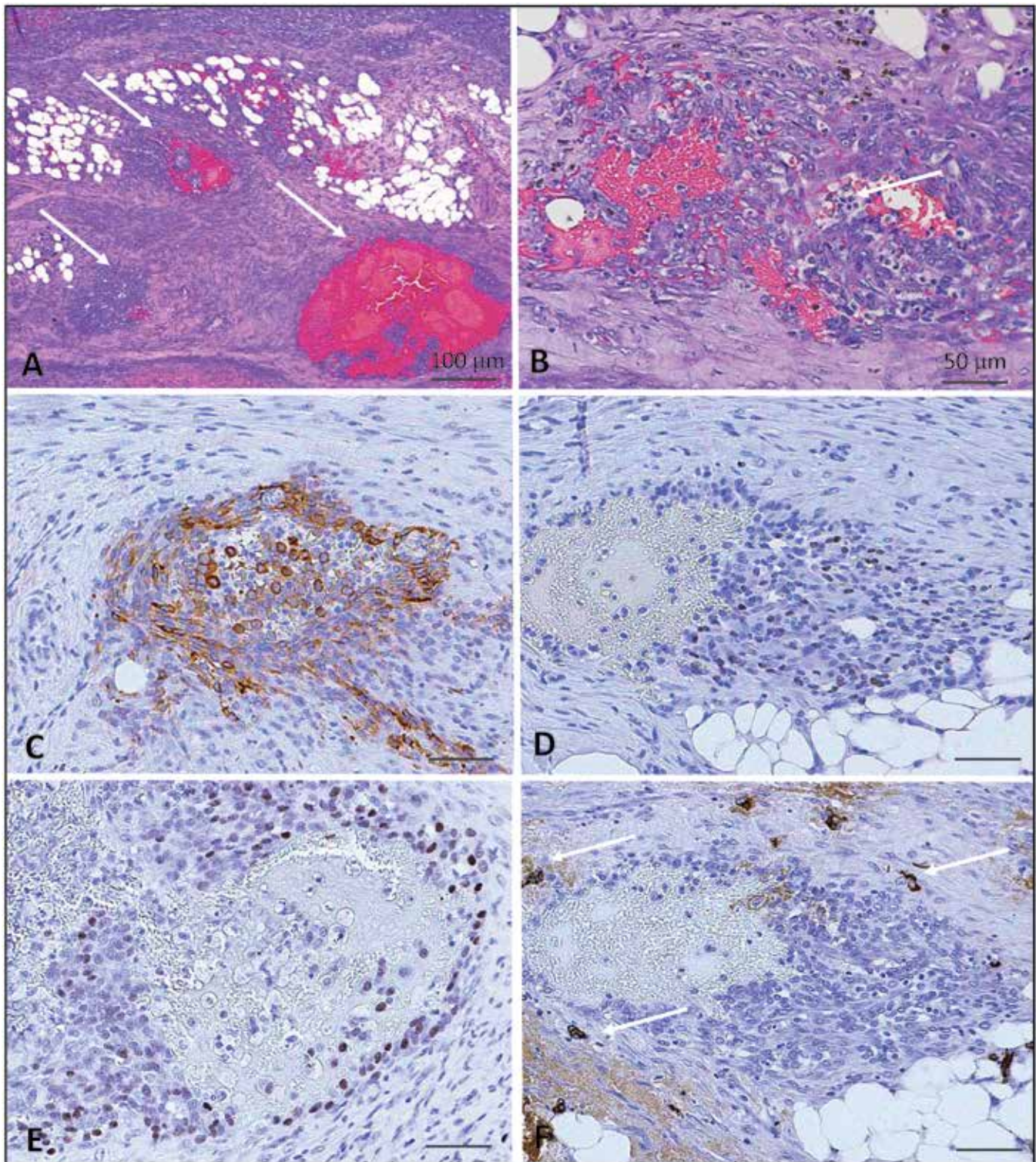


Figure 3. Peritoneal pathology. (A) Representative section of peritoneal proliferative lesions. Numerous variably sized blood-filled cystic structures (arrows) are embedded within fibrovascular proliferative tissue that coated serosal surfaces and dissected through omental fat. These structures are illustrated in increased detail in panels B through F. Hematoxylin and eosin stain. (B) Blood-filled cystic structures are lined by spindle-shaped to polygonal cells with central necrosis (arrow). Hematoxylin and eosin stain. (C through E) Cells enclosing blood-filled spaces express (C) CD10, (D) estrogen receptor, and (E) progesterone receptor. (F) These regions fail to express FVIII-Rag, a reaction that is evident in surrounding vascular profiles (arrows). Bar, 100 μ m (A); 50 μ m (B through F).

clinical signs are cyclical anorexia, depression, heavy bleeding, constipation, palpable abdominal masses, and reproductive failure.^{1,10,12} Retrograde menstruation is considered to be the primary mechanism of transplantation of ectopic endometrial tissue.^{1,20} This tissue can be found anywhere in the body, causing

site-specific symptoms.^{12,24} Most commonly, the ectopic endometrial tissue causes abnormalities in the pelvic region secondary to endometrial cysts and adhesions involving the reproductive, gastrointestinal, or urinary tracts.^{1,12,24} In humans, intestinal endometriosis is a rare condition that typically presents as focal

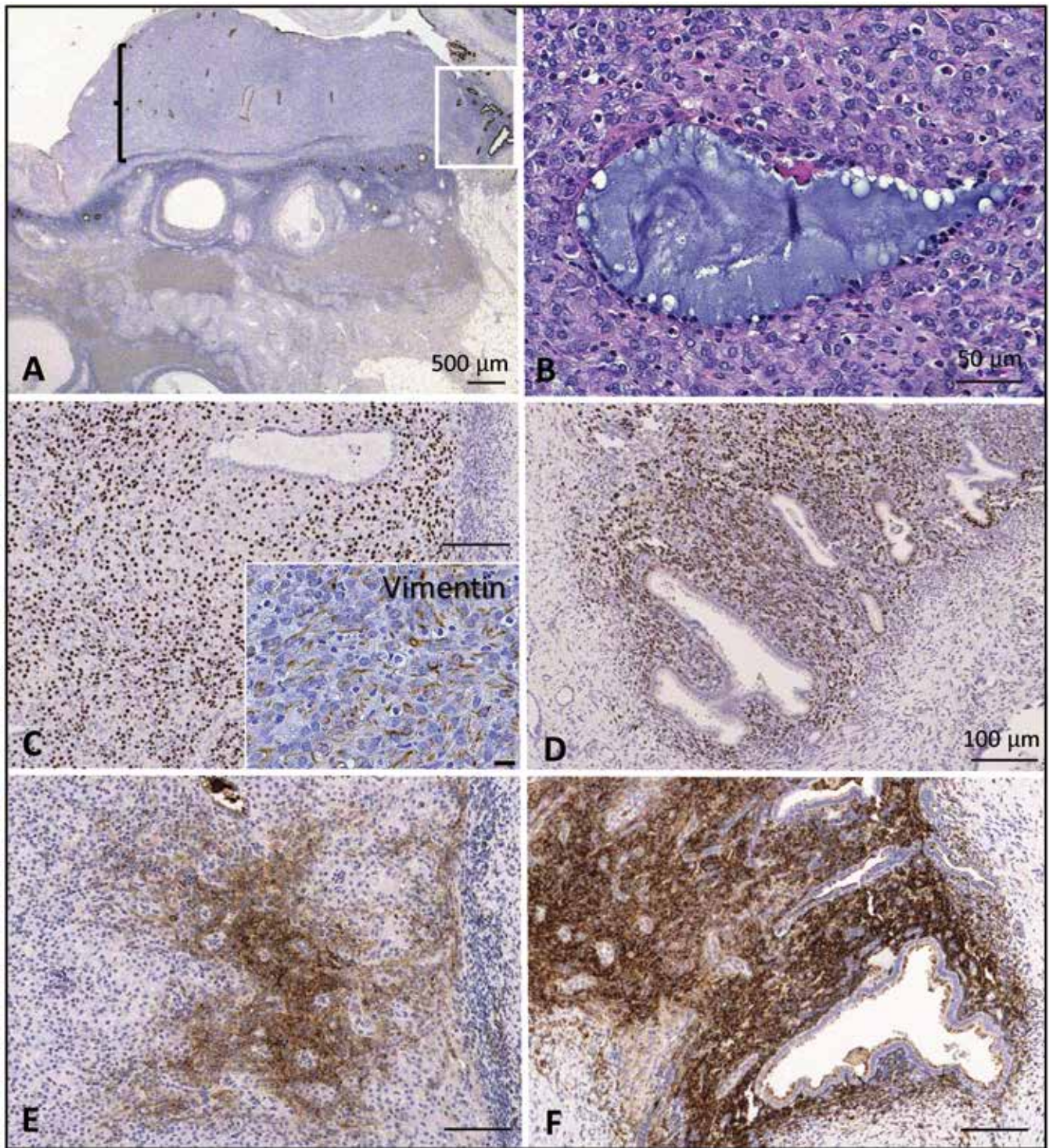


Figure 4. Ovarian pathology. (A) Both ovaries are enclosed in a 0.5- to 2-mm thick coat of tissue (indicated by parentheses) that is continuous with regions of ovarian endometriosis (white rectangle). Glandular profiles in both of these regions are immunopositive for broad-spectrum cytokeratin (immunohistochemistry, cytokeratin AE1/AE3). (B) Periovarian tissue is composed predominantly of spindle-shaped to polygonal cells with prominent cytoplasm, clear cytoplasmic borders, and minimal cellular atypia. Embedded within this tissue are rare glandular structures lined by simple cuboidal to columnar epithelium, which occasionally contain mucinous secretions. Hematoxylin and eosin stain. Periovarian tissue is vimentin-positive (inset, C) and strongly immunopositive for progesterone receptor (nuclear staining, E). (D and F) A region of periovarian endometriosis (white rectangle in A) displays strong stromal immunoreactivity for progesterone receptor (nuclear staining, D) and CD10 (cytoplasmic staining, F). Bar, 500 μ m (A); 50 μ m (B); 100 μ m (C through F); 20 μ m (inset, C).

bowel lesions that occasionally can result in intestinal obstruction.^{16,28} Bowel obstruction secondary to endometriosis in NHP has not been reported previously. The severity of the peritoneal response in our macaque was considered to be unusually

excessive for sole diagnosis of endometriosis. Furthermore, we were unable to demonstrate clearly differentiated epithelial and stromal components characteristic of this lesion. Extragenital ESS in humans has been described affecting a variety

Table 1. Comparative immunohistochemistry of endometriotic ovarian and peritoneal lesions

| Target | Antibody ^a | Positive control | Periovarian tissue | | Endometriosis | | Peritoneal tumor (cystic masses) |
|-----------------------|--------------------------------|-----------------------------|--------------------|------------|---------------|------------|----------------------------------|
| | | | Stromal | Epithelial | Stromal | Epithelial | |
| AE1/AE3 | ms343, Neomarkers; 1:100 | Epithelium, oviduct | – | + | – | + | – |
| CK5/6 | m7237, Dako; 1:160 | Epithelium, oviduct | – | – | – | + | – |
| Smooth-muscle actin | ms113, Neomarkers; 1:1500 | Stroma, vasculature oviduct | + | Rare + | + | Rare + | + |
| CD10 | ms728, Thermo Scientific; 1:30 | Stroma, endometrium | + | Apical + | + | Apical + | + |
| Wilm tumor 1 | m3561, Dako; 1:50 | Granulosa cells, ovary | + | – | + | – | + |
| Estrogen receptor | m7047, Dako; 1:50 | Stroma, epithelium, oviduct | Rare + | Rare + | + | + | + |
| Progesterone receptor | crm302, Biocare; 1:100 | Stroma, epithelium, oviduct | + | + | + | + | + |
| c-kit | A4502, Dako; 1:200 | Myenteric plexus | – | – | – | – | – |
| Calretinin | m7245, Dako; 1:50 | Retina, amacrine cells | – | – | – | – | – |

Positive control tissue was taken from the same animal.

^aCatalog number, manufacturer (Neomarkers, Fremont, CA; Dako, Santa Clara, CA; Thermo Scientific, Waltham, MA; Biocare, Yorba Linda, CA), dilution.

of peritoneal organs^{3,6,19} and arising from ovarian²¹ or extragonadal endometriotic lesions.^{7,18} Histologically, ESS tumors are typically composed of sheets of cells resembling endometrial stroma, prominent stromal vascularity, few mitotic figures, and mild cellular atypia. ESS lesions invariably express CD10, estrogen receptor, and progesterone receptor.^{6,19} These histologic and immunohistochemical characteristics are consistent with those identified in our case and support a diagnosis of ESS.

In humans, as in our NHP case, ESS most commonly presents with symptoms of intestinal obstruction.^{7,18} Terminal clinical signs in this macaque were consistent with acute intestinal obstruction, initially indistinguishable from those accompanying gastric dilatation. However, subsequent clinical and radiographic findings implicated the lower intestinal tract as a more likely source of obstruction. Large intestinal distortion by an extraintestinal fibrovascular proliferative reaction was confirmed at necropsy. Histologic and immunohistochemical findings, as well as the concurrent well-differentiated endometriotic foci distributed throughout proliferative tissue, support our conclusion that the florid fibrovascular peritoneal proliferation originated from the stromal tissue of endometrial origin. The florid nature and relatively poor differentiation of this lesion favor selection of ESS rather than endometriosis as the most likely diagnosis. To our knowledge, this report is the first description in an NHP of an entity that resembles clinical and histologic features of ESS in humans.

References

1. Abee CR, Mansfield K, Tardif S, Morris T, editors. 2012. Nonhuman primates in biomedical research, 2nd ed. Amsterdam (Netherlands): Academic Press.
2. Akbulut S. 2015. Accurate definition and management of idiopathic sclerosing encapsulating peritonitis. *World J Gastroenterol* 21:675–687. <https://doi.org/10.3748/wjg.v21.i2.675>.
3. Alcázar JL, Guerriero S, Ajossa S, Parodo G, Piras B, Peiretti M, Jurado M, Idoate MÁ. 2012. Extragenital endometrial stromal sarcoma arising in endometriosis. *Gynecol Obstet Invest* 73:265–271. <https://doi.org/10.1159/000336522>.
4. Altman AD, Bentley JR, Rittenberg PV, Murray SK. 2016. Luteinized thecomas ('thecomatosis') with sclerosing peritonitis (LTSP): report of 2 cases and review of an enigmatic syndrome associated with a peritoneal proliferation of specialized (vimentin⁺/keratin⁺/CD34⁺) submesothelial fibroblasts. *J Obstet Gynaecol Can* 38:41–50.
5. Bennett BT, Cuasay L, Welsh TJ, Beluhan FZ, Schofield L. 1980. Acute gastric dilatation in monkeys: a microbiologic study of gastric contents, blood, and feed. *Lab Anim Sci* 30:241–244.
6. Biliatis I, Akrivos N, Sotiropoulou M, Rodolakis A, Simou M, Antsaklis A. 2012. Endometrial stromal sarcoma arising from endometriosis of the terminal ileum: the role of immunohistochemistry in the differential diagnosis. *J Obstet Gynaecol Res* 38:899–902. <https://doi.org/10.1111/j.1447-0756.2011.01783.x>.
7. Budäus LH, Menzel T, Hartmann V, Caselitz J, Doerner A. 2008. Acute abdomen caused by endometrial stromal sarcoma arising in extragonadal foci of endometriosis of the terminal ileum. *Int J Colorectal Dis* 23:447–448. <https://doi.org/10.1007/s00384-007-0361-4>.
8. Christie RJ, King RE. 1981. Acute gastric dilation and rupture in *Macaca arctoides* associated with *Clostridium perfringens*. *J Med Primatol* 10:263–264. <https://doi.org/10.1159/000460083>.
9. Churg A, Galateau-Salle F. 2012. The separation of benign and malignant mesothelial proliferations. *Arch Pathol Lab Med* 136:1217–1226. <https://doi.org/10.5858/arpa.2012-0112-RA>.
10. Connolly MA, Trentalange M, Zeiss CJ. 2016. Long-term clinical outcomes in diabetic rhesus macaques (*Macaca mulatta*) treated with medroxyprogesterone acetate for endometriosis. *Comp Med* 66:343–348.
11. Cruzen CL, Baum ST, Colman RJ. 2011. Glucoregulatory function in adult rhesus macaques (*Macaca mulatta*) undergoing treatment with medroxyprogesterone acetate for endometriosis. *J Am Assoc Lab Anim Sci* 50:921–925.
12. Fanton JW, Hubbard GB, Wood DH. 1986. Endometriosis: clinical and pathologic findings in 70 rhesus monkeys. *Am J Vet Res* 47:1537–1541.
13. Giddens WE Jr, Tsai CC, Morton WR, Ochs HD, Knitter GH, Blakley GA. 1985. Retroperitoneal fibromatosis and acquired immunodeficiency syndrome in macaques. Pathologic observations and transmission studies. *Am J Pathol* 119:253–263.
14. Heerkens TM, Smith JD, Fox L, Hostetter JM. 2011. Peritoneal fibrosarcomatous mesothelioma in a cat. *J Vet Diagn Invest* 23:593–597. <https://doi.org/10.1177/1040638711403405>.
15. Kahn HS, Curtis KM, Marchbanks PA. 2003. Effects of injectable or implantable progestin-only contraceptives on insulin–glucose metabolism and diabetes risk. *Diabetes Care* 26:216–225. <https://doi.org/10.2337/diacare.26.1.216>.
16. Khwaja SA, Zakaria R, Carneiro HA, Khwaja HA. 2012. Endometriosis: a rare cause of small bowel obstruction. *BMJ Case Rep* 2012:1–4.
17. Kim KM, Lee SR, Chang KS, Lee YH, Kim SW, Jung KJ, Lee Y, Kim D, Chang KT. 2012. Acute gastrointestinal dilation in laboratory rhesus monkeys in the Korea National Primate Research Center. *Lab Anim Res* 28:217–221. <https://doi.org/10.5625/lar.2012.28.3.217>.
18. Kovac D, Gasparović I, Jasic M, Fuckar D, Dobi-Babić R, Haller H. 2005. Endometrial stromal sarcoma arising in extrauterine endometriosis: a case report. *Eur J Gynaecol Oncol* 26:113–116.

19. **Lan C, Huang X, Lin S, Cai M, Liu J.** 2012. Endometrial stromal sarcoma arising from endometriosis: a clinicopathological study and literature review. *Gynecol Obstet Invest* **74**:288–297. <https://doi.org/10.1159/000341706>.
20. **Lindberg BS, Busch C.** 1984. Endometriosis in rhesus monkeys. *Ups J Med Sci* **89**:129–134. <https://doi.org/10.3109/03009738409178472>.
21. **Mitchard JR, Lott M, Afifi RA, Hirschowitz L.** 2004. Low-grade endometrial stromal sarcoma with glandular differentiation arising in ovarian endometriosis. *J Obstet Gynaecol* **24**:596–597. <https://doi.org/10.1080/01443610410001722879>.
22. **Newton WM, Beamer PD, Rhoades HE.** 1971. Acute bloat syndrome in stumptailed macaques (*Macaca arctoides*): a report of 4 cases. *Lab Anim Sci* **21**:193–196.
23. **Pond CL, Newcomer CE, Anver MR.** 1982. Acute gastric dilatation in nonhuman primates: review and case studies. *Vet Pathol Suppl* **19 Suppl** 7:126–133. <https://doi.org/10.1177/030098588201907s09>.
24. **Schaerdel AD.** 1986. Pelvic endometriosis associated with infarctions of the colon in a rhesus monkey. *Lab Anim Sci* **36**:533–536.
25. **Soave OA.** 1978. Observations on acute gastric dilatation in nonhuman primates. *Lab Anim Sci* **28**:331–334.
26. **Staats PN, McCluggage WG, Clement PB, Young RH.** 2008. Luteinized thecomas (thecomatosis) of the type typically associated with sclerosing peritonitis: a clinical, histopathologic, and immunohistochemical analysis of 27 cases. *Am J Surg Pathol* **32**:1273–1290. <https://doi.org/10.1097/PAS.0b013e3181666a5f>.
27. **Tandon R, Jimenez-Cortez Y, Taub R, Borczuk AC.** 2017. Immunohistochemistry in peritoneal mesothelioma: a single-center experience of 244 cases. *Arch Pathol Lab Med* **142**:236–242. doi:10.5858/arpa.2017-0092-OA.
28. **Torralba-Morón A, Urbanowicz M, Ibarrola-De Andres C, Lopez-Alonso G, Colina-Ruizdelgado F, Guerra-Vales JM.** 2016. Acute small bowel obstruction and small bowel perforation as a clinical debut of intestinal endometriosis: a report of 4 cases and review of the literature. *Intern Med* **55**:2595–2599. <https://doi.org/10.2169/internalmedicine.55.6461>.
29. **Westmoreland SV, Mansfield KG.** 2008. Comparative pathobiology of Kaposi sarcoma-associated herpesvirus and related primate rhadinoviruses. *Comp Med* **58**:31–42.
30. **Zondervan KT, Weeks DE, Colman R, Cardon LR, Hadfield R, Schleffler J, Trainor AG, Coe CL, Kemnitz JW, Kennedy SH.** 2004. Familial aggregation of endometriosis in a large pedigree of rhesus macaques. *Hum Reprod* **19**:448–455. <https://doi.org/10.1093/humrep/deh052>.